

****Volume Title****

ASP Conference Series, Vol. **Volume Number**

****Author****

© **Copyright Year Astronomical Society of the Pacific**

Modelling H₂ Infrared Emission of the Helix Nebula Cometary Knots

Isabel Aleman^{1,2}, Albert A. Zijlstra¹, Mikako Matsuura^{3,4}, Ruth Gruenwald², and Rafael Kimura²

¹*Jodrell Bank Centre for Astrophysics, The Alan Turing Building, School of Physics and Astronomy, The University of Manchester, Oxford Rd, Manchester, M13 9PL, UK*

²*IAG-USP, Universidade de São Paulo, Cidade Universitária, Rua do Matão 1226, São Paulo, SP, 05508-090, Brazil*

³*UCL-Institute of Origins, Astrophysics Group, Department of Physics and Astronomy, University College London, Gower Street, London, WC1E 6BT, UK*

⁴*UCL-Institute of Origins, Mullard Space Science Laboratory, University College London, Holmbury St. Mary, Dorking, Surrey, RH5 6NT, UK*

Abstract. In the present work, we use a photoionisation code to study the H₂ emission of the Helix nebula (NGC 7293) cometary knots, particularly that produced in the interface H⁺/H⁰ of the knot, where a significant fraction of the H₂ 1-0 S(1) emission seems to be produced. Our results show that the production of molecular hydrogen in such region may explain several characteristics of the observed emission, particularly the high excitation temperature of the H₂ infrared lines.

1. Introduction

High-resolution images of the Helix nebula (NGC 7293) have shown that the H₂ emission arises from its large population of dense globules embedded in the ionised gas (e.g. Matsuura et al. 2009), the so-called cometary knots (CKs). CKs are structures that resemble comets, particularly in images taken in H α , [N II] λ 6583, and H₂ 1-0 S(1) lines. The bright cusp points towards the central star and the tail in the opposite direction, which can indicate that the excitation is connected with the central star (O'Dell et al. 2005, 2007).

The H₂ emission is intense in a thin layer on the surface of the CKs towards the central star. There is no evidence that this emission is produced by shocks (O'Dell et al. 2005; Matsuura et al. 2007). Models of photodissociation regions (PDRs; Cox et al. 1998; O'Dell et al. 2007) are unable to reproduce the high excitation temperature of H₂ emission (\sim 900-1800 K) estimated by Cox et al. (1998) and Matsuura et al. (2007). Recently, Henney et al. (2007) showed that advection can cause the ionisation and dissociation front to merge, leading to enhanced heating of the molecular gas.

In this work, we show that the partially ionised region can account for a significant part of the observed H₂ emission and naturally explain its high excitation temperature. Our models are briefly described in Section 2; a more detailed description will be pub-

lished in a forthcoming paper (Aleman et al. 2010). Results are presented in Section 3.

2. Models

We use the photoionisation code *Aangaba* (Gruenwald & Viegas 1992) to simulate the ionising spectrum, physical conditions, density of the species, and line emissivities around and inside the H^+/H^0 interface of the Helix nebula CKs. The H_2 micro-physics is included in the code, as described in Aleman & Gruenwald (2004, 2010).

We assume that the central star radiates as a blackbody with $T_\star = 120,000$ K and $L_\star = 100 L_\odot$ (Henry et al. 1999; O’Dell et al. 2007). We also assume that the density of the diffuse gas is uniform and equal to 50 cm^{-3} (Meixner et al. 2005). The elemental abundances for the Helix were determined by Henry et al. (1999) for He, O, C, N, Ne, S, and Ar. For Mg, Si, Cl, and Fe, we adopt averages for PNe from Stasińska & Tylenda (1986). We use amorphous carbon dust (with $0.1 \mu\text{m}$ radius) for our calculations, but as discussed in Aleman & Gruenwald (2004) the choice of compound among the ones available in the code will not cause significant changes on the results presented below nor will affect our conclusions. The distance to the Helix is assumed to be 219 pc (Harris et al. 2007). The CKs are simulated as an increase in the density profile of the Helix nebula model at a given distance from the central star. The emissivity along the radial direction (through the CK symmetry axis) is calculated by the photoionisation code. An IDL routine was developed to simulate a three-dimensional CK, allowing the calculation of line surface brightness by the integration of the emissivity in the line of sight inside a CK, which is assumed to be seen edge on. We construct a grid of CK models with different core densities, density profiles, dust-to-gas ratios, and distances from the central star. We assume that the density profile has a density increase from the diffuse gas to the CK core value within a given distance. We call this region the CK interface. We study four types of density increase with distance, but here we only present the results for the exponential increase (more results will be included in Aleman et al. 2010). Calculation are stopped where the gas temperature, which generally decreases with the distance to the central star, reaches 100 K. In each model, the dust-to-gas ratio and the chemical composition of the CKs are assumed to be the same as in the diffuse gas.

3. Results

3.1. Warm H_2 1-0 S(1) emission

The emissivity of the H_2 1-0 S(1) line, as well as for other rovibrational lines, in the CKs is important in a warm region, where temperatures are between 300 and 7000 K. In the region considered in this work, the peak in the 1-0 S(1) emissivity occurs where the density is around 40% of the core density. The contribution of colder regions should be more important for pure rotational lines of the $v = 0$ level. This component of the H_2 emission may explain the excitation temperatures around 900-1800 K found by Cox et al. (1998) and Matsuura et al. (2007).

The left panel in Fig. 1 shows the H_2 excitation diagram. Observational values were obtained by Matsuura et al. (2007). Values calculated with an appropriate model are also included. The agreement between the excitation temperatures of the model and

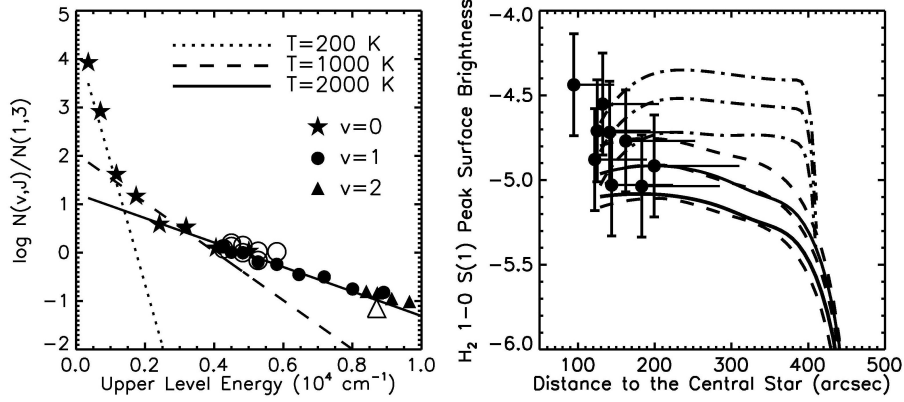


Figure 1. Left Panel: H_2 excitation diagram. The effective column density was calculated where the 1-0 S(1) surface brightness is maximum. Open symbols represents observations and filled symbols models. Lines are Boltzmann distributions for the temperature indicated. Right panel: H_2 1-0 S(1) surface brightness of a cometary knot as a function of its distance to the central star. Sets of solid, dashed, and dot-dashed curves represent models with interface thickness of 0.5, 0.2, and 0.01'', respectively. Different curves within each set represent CK radius of 0.5, 1.0, and 2.0'', with the surface brightness increasing for larger CK radius. Dots represent measured values. The error in the distance is estimated assuming that the Helix symmetry axis is inclined 37° with respect to the line of sight

the observations is evident. Lines represent Boltzmann distributions for three different temperatures as indicated within the plot. The column densities obtained from the lines of the bands 1-0 and 2-1 are well represented by a excitation temperature of approximately 2000 K. A similar value was obtained by Matsuura et al. (2007). The column densities obtained from lines 0-0 S(2) to S(7) are well represented by Boltzmann distribution at a temperature of 1000K, which is close to the excitation temperature of 900K obtained by Cox et al. (1998) from ISO observations of the Helix.

3.2. H_2 1-0 S(1) surface brightness

The right panel of Fig. 1 shows the H_2 1-0 S(1) line surface brightness as a function of the CK distance to the central star. Dots represent measurements for some representative CKs of the Helix nebula. We identified 10 isolated CKs commonly detected in $H\alpha$ and H_2 images. We measured $2.12 \mu\text{m}$ H_2 intensities from the images obtained by Matsuura et al. (2009). To calibrate the data for point sources on the local scale, we use five stars within the observed field to measure the zero-point. We assume that the 2MASS K' -magnitude of these stars are the same as the magnitudes in H_2 -filter. We apply the 25-pixel radius of aperture photometry and take the 35–50 pixel ring as background measurements. The pixel scale is $0.117''$.

Curves in the right panel of Fig. 1 show the H_2 1-0 S(1) surface brightness as a function of the distance from the central star for CKs with different interface thickness and radius. The surface brightness was calculated was averaged over the same aperture as the measurements to allow direct comparison. The surface brightness decreases with the decrease of interface thickness, the increase of the CK radius, and the increase of the distance from the central star. The observed surface brightness also presents a decrease

with distance to the central star trend. The interface can account for the whole or a significant part of the observed surface brightness.

An important parameter to the ionization structure of the CKs is the distance from the central star, since the ionising spectrum may change significantly with the optical depth. CKs farther from the central star have smaller ionised zones. If the CK is beyond the Helix ionisation front, there is practically no ionised region and the intensity of 1-0 S(1) drops dramatically, since there is not enough radiation or temperature to excite significantly the upper vibrational levels of the molecule. Our results support that the central star's radiation field plays a major role in the CKs H₂ emission.

We also study the effect of the dust-to-gas ratio and n_K . The 1-0 S(1) peak brightness is slightly higher for models with higher dust-to-gas ratio (the increase caused by changing the dust-to-gas ratio from 10^{-3} to 10^{-2} is about 20%) and higher n_K (the difference between models with $n_K = 10^5$ and 10^6 cm⁻³ is up to 40%).

As pointed out by Burkert & O'Dell (1998), the interface between the diffuse gas and the CK core may provide important clues about the mechanisms that shapes and sustain the CKs. Our models show that there are significant differences in the results depending on the assumed density profiles of this region. Images that could resolve the interface of the CK in great detail are then essential to improve or knowledge about the CKs and PNe.

Acknowledgments. We acknowledge the financial support from CNPq PDE grant number 201950/2008-1 (Brazil), The University of Manchester, and STFC (UK).

References

- Aleman, I., & Gruenwald, R. 2004, *ApJ*, 607, 865. [arXiv:astro-ph/0403189](#)
— 2010, *A&A*. Submitted
Aleman, I., Zijlstra, A. A., Matsuura, M., Gruenwald, R., & Kimura, R. 2010, *MNRAS*. In preparation
Burkert, A., & O'Dell, C. R. 1998, *ApJ*, 503, 792
Cox, P., Boulanger, F., Huggins, P. J., Tielens, A. G. G. . M., Forveille, T., Bachiller, R., Cesarsky, D., Jones, A. P., Young, K., Roelfsema, P. R., & Cernicharo, J. 1998, *ApJ*, 495, L23+
Gruenwald, R. B., & Viegas, S. M. 1992, *AJS*, 78, 153
Harris, H. C., Dahn, C. C., Canzian, B., Guetter, H. H., Leggett, S. K., Levine, S. E., Luginbuhl, C. B., Monet, A. K. B., Monet, D. G., Pier, J. R., Stone, R. C., Tilleman, T., Vrba, F. J., & Walker, R. L. 2007, *AJ*, 133, 631. [arXiv:astro-ph/0611543](#)
Henney, W. J., Williams, R. J. R., Ferland, G. J., Shaw, G., & O'Dell, C. R. 2007, *ApJ*, 671, L137. [0711.4334](#)
Henry, R. B. C., Kwitter, K. B., & Dufour, R. J. 1999, *ApJ*, 517, 782. [arXiv:astro-ph/9901060](#)
Matsuura, M., Speck, A. K., McHunu, B. M., Tanaka, I., Wright, N. J., Smith, M. D., Zijlstra, A. A., Viti, S., & Wesson, R. 2009, *ApJ*, 700, 1067. [0906.2870](#)
Matsuura, M., Speck, A. K., Smith, M. D., Zijlstra, A. A., Viti, S., Lowe, K. T. E., Redman, M., Wareing, C. J., & Lagarde, E. 2007, *MNRAS*, 382, 1447. [0709.3065](#)
Meixner, M., McCullough, P., Hartman, J., Son, M., & Speck, A. 2005, *AJ*, 130, 1784. [arXiv:astro-ph/0509887](#)
O'Dell, C. R., Henney, W. J., & Ferland, G. J. 2005, *AJ*, 130, 172. [arXiv:astro-ph/0504210](#)
— 2007, *AJ*, 133, 2343. [arXiv:astro-ph/0701636](#)
Stasińska, G., & Tylenda, R. 1986, *A&A*, 155, 137